Biophysical Journal
Article

Biophysical Society

How Tim proteins differentially exploit membrane features to attain robust target sensitivity

Daniel Kerr,[1,2,3] Zhiliang Gong,[2,3] Tiffany Suwatthee,[2] Adrienne Luoma,[4] Sobhan Roy,[5] Renee Scarpaci,[6] Hyeondo Luke Hwang,[2,3] J. Michael Henderson,[2,3] Kathleen D. Cao,[2,3] Wei Bu,[7] Binhua Lin,[3,7] Gregory T. Tietjen,[8] Theodore L. Steck,[5] Erin J. Adams,[1,4,5] and Ka Yee C. Lee[1,2,3,*]

[1]Program in Biophysical Sciences, Institute for Biophysical Dynamics, [2]Department of Chemistry, [3]James Franck Institute, [4]Committee on Immunology, and [5]Department of Biochemistry and Molecular Biology, The University of Chicago, Chicago, Illinois; [6]City University of New York City College, New York, New York; [7]NSF's ChemMatCARS, The University of Chicago, Chicago, Illinois; and [8]Department of Surgery, Section of Transplant and Immunology and Department of Biomedical Engineering, Yale University, New Haven, Connecticut

ABSTRACT Immune surveillance cells such as T cells and phagocytes utilize integral plasma membrane receptors to recognize surface signatures on triggered and activated cells such as those in apoptosis. One such family of plasma membrane sensors, the transmembrane immunoglobulin and mucin domain (Tim) proteins, specifically recognize phosphatidylserine (PS) but elicit distinct immunological responses. The molecular basis for the recognition of lipid signals on target cell surfaces is not well understood. Previous results suggest that basic side chains present at the membrane interface on the Tim proteins might facilitate association with additional anionic lipids including but not necessarily limited to PS. We, therefore, performed a comparative quantitative analysis of the binding of the murine Tim1, Tim3, and Tim4, to synthetic anionic phospholipid membranes under physiologically relevant conditions. X-ray reflectivity and vesicle binding studies were used to compare the water-soluble domain of Tim3 with results previously obtained for Tim1 and Tim4. Although a calcium link was essential for all three proteins, the three homologs differed in how they balance the hydrophobic and electrostatic interactions driving membrane association. The proteins also varied in their sensing of phospholipid chain unsaturation and showed different degrees of cooperativity in their dependence on bilayer PS concentration. Surprisingly, trace amounts of anionic phosphatidic acid greatly strengthened the bilayer association of Tim3 and Tim4, but not Tim1. A novel mathematical model provided values for the binding parameters and illuminated the complex interplay among ligands. In conclusion, our results provide a quantitative description of the contrasting selectivity used by three Tim proteins in the recognition of phospholipids presented on target cell surfaces. This paradigm is generally applicable to the analysis of the binding of peripheral proteins to target membranes through the heterotropic cooperative interactions of multiple ligands.

SIGNIFICANCE Many receptors on the plasma membranes of immune surveillance cells recognize molecular signatures on target cell surfaces. However, these intercellular recognition mechanisms are not well understood. We characterized the binding of the murine transmembrane immunoglobulin and mucin domain (Tim) family of proteins, Tim1, Tim3, and Tim4, to phospholipid vesicles that mimic apoptotic cells using a combination of structural, biochemical, and theoretical approaches. The three murine homologs differed in their utilization of calcium coordination, electrostatic contacts, and hydrophobic interactions to robustly, sensitively, and selectively target phospholipid signatures characteristic of apoptotic membranes. The mathematical model we developed to depict these interactions is generally applicable to heterogeneous interactions between membranes and peripheral proteins.

INTRODUCTION

Many peripheral proteins target the outer or inner surface of plasma membranes (1–3). Often, these proteins utilize cooperative interactions involving different ligands to confer strength and selectivity (4). The protein interface with the membrane can be viewed as a multidentate contact surface. The diversity of plasma membrane lipids and the multiplicity of protein-lipid interactions have made it difficult to parse the physiological role of such interactions (1). We therefore undertook a comparative characterization of the membrane association of three immune surveillance homologs: transmembrane immunoglobulin and mucin domain mouse proteins (Tim) 1, Tim3, and Tim4 (5). These Tim proteins share a highly conserved lipid-binding domain but each plays a different immunological role. We investigated how these

Submitted February 2, 2021, and accepted for publication September 8, 2021.

*Correspondence: kayeelee@uchicago.edu

Daniel Kerr and Zhiliang Gong contributed equally to this work.

Editor: Michael Brown.

https://doi.org/10.1016/j.bpj.2021.09.016

proteins associate with phospholipid membranes and how their binding is tuned by various membrane features. Our findings potentially provide a link between the distinct immunological functions of each Tim protein and their differential sensitivities for target membranes.

The Tims are ~40 kDa plasma membrane proteins comprised of a projecting N-terminal immunoglobulin (Ig) domain (~13 kDa), a mucin domain at the plasma membrane surface, a single-pass transmembrane domain and a C-terminal tail that bears a phosphorylated tyrosine and interacts with several cytoplasmic effectors (5–9). All three are expressed in both a full, plasma-membrane-anchored form and a truncated, water-soluble form (10,11). Cells bearing Tim1, Tim3, or Tim4 recognize triggered cells, such as those undergoing apoptosis (12,13), though the three proteins serve different and even opposing physiological roles (5). Tim1 is a positive effector of T cell immunity (14). Tim3 serves as an immune checkpoint receptor on the surface of a variety of T cells and macrophages (6,7); it downregulates immune processes by, for example, suppressing autoimmune and alloimmune responses and promoting peripheral immune tolerance. Tim4 mediates the attack of macrophages and other phagocytes on apoptotic T cells (9,13–16).

Tim surveillance involves the recognition of molecular signatures on target cell surfaces (17–23). Phosphatidylserine (PS) is a prime target. Individual PS headgroups coordinate through a calcium ion link with polar and charged side chains in the "central pocket" of a projecting Ig domain of a Tim protein to form Tim-Ca^{2+}-PS ternary linkages (5,15,24–28). In addition to this central pocket that has been reported to be specific for PS, additional PS molecules strengthen binding by engaging electrostatically with the basic side chains adjoining the central pocket (15). However, these peripheral basic side chains could be sensitive to charges at the membrane besides PS, such as other anionic phospholipids. PS is normally sequestered in the inner leaflet of the highly asymmetric plasma membrane bilayer, driven by ATP-dependent flippases (29,30). Apoptotic and other pathophysiological signals trigger the flux of extracellular calcium ions into the cytoplasm and activate a scramblase that conveys anionic inner leaflet phospholipids to the extracellular surface (29,31–33). These not only include PS but also phosphatidic acid (PA), phosphatidylglycerol (PG), phosphatidylinositol, and its derivatives. The surface exposure of these anionic lipids has been thought to promote Tim binding and, consequently, diverse homeostatic responses (28,29,34).

The physicochemical basis for Tim proteins recognition of different target cell surfaces is poorly understood (28). Of itself, PS binding alone does not account for the selectivity of the Tim proteins or other PS receptors. We therefore characterized the binding of the water-soluble Ig domains of mouse Tim1, Tim3, and Tim4 to large unilamellar vesicles containing different anionic phospholipids to help elucidate the selectivity of Tim protein binding. We investigated the influence of several likely elements in the molecular recognition of apoptotic membranes: anionic lipids PS, PA, and PG, calcium ions, hydrophobic interactions, and fatty acyl chain unsaturation. A molecular model for Tim3 binding to the lipid membrane derived from x-ray reflectivity data was compared with similar structures obtained for Tim1 and Tim4, providing a guide to biochemical experiments (14,35). Given the complex interplay of the various ligands in the binding, capturing the multiligand dependence properly necessitated the development of a new model to analyze these interactions (36). This formulation enabled the extraction of values for the binding parameters, showing that the three Tim proteins employ the same kinds of mechanisms for their association with bilayers but balance them differently to achieve distinctive binding behavior. Surprisingly, the presence of small amounts of PA in PS-containing membranes greatly strengthened the binding of Tim3 and Tim4. Tim3 has been assigned a minimal role in membrane recognition (37). However, our results suggest that this protein may be as strong a sensor of apoptotic cells as Tim1 and Tim4.

MATERIALS AND METHODS

Recombinant Tim1, Tim3, and Tim4 were produced in Hi5 cells via baculovirus transfection (38). Large unilamellar phospholipid vesicles were obtained by extrusion (39). X-ray reflectivity experiments utilized monolayer films composed of mixtures containing mixtures of PC/PS = 7:3 with 1-stearoyl-2-oleoyl chains. Tim protein binding was determined from tryptophan fluorescence spectra (14,35). All data points represent the averages of at least three independent experiments. See the Supporting materials and methods for details.

RESULTS

A molecular model for Tim-membrane binding

We previously obtained membrane-bound orientations of Tim1 and Tim4 (14,35). However, only the crystal structure of the soluble Ig domain of Tim3 was known (26). We therefore used x-ray reflectivity to characterize the disposition of this Tim3 domain on a lipid monolayer composed of 70 mol % 1-stearoyl-2-oleoyl-sn-glycero-3-phosphocholine and 30 mol% 1-stearoyl-2-oleoyl-sn-glycero-3-phospho-L-serine, the lipid composition used in the aforementioned analysis of Tim1 and Tim4 (Fig. S1). The disposition of Tim3 on the membrane was compared to that previously obtained for Tim1 and Tim4 (Fig. 1). Three principal modes of interaction were identified: a Tim-Ca^{2+}-PS link (Ca^{2+} represented as a *yellow sphere*), electrostatic engagement of basic side chains with anionic phospholipid headgroups (colored in *red* and *green*), and the insertion of hydrophobic side chains into the region of the phospholipid tails (colored in *gray*). This structural analysis guided our study of the binding of these three proteins to anionic phospholipid vesicles with features characteristic of apoptotic plasma membranes.

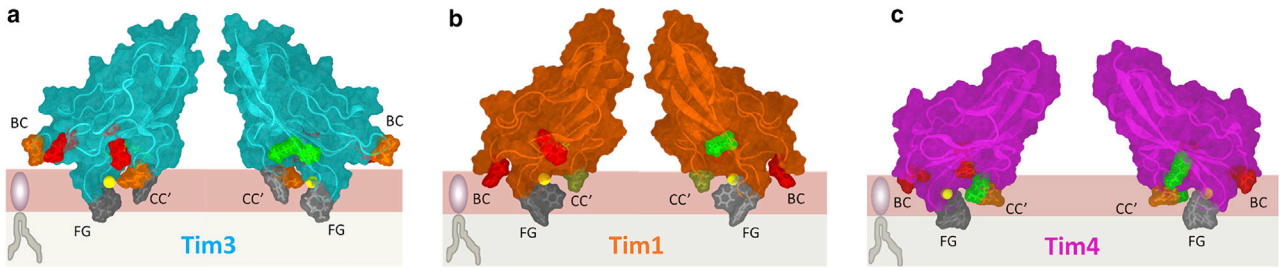

FIGURE 1 Association of Tim proteins with PS-containing phospholipid membranes. Each monolayer was composed of a 7:3 mixture of PC/PS containing 1-stearoyl-2-oleoyl chains. The top (*pink*) stratum represents the headgroup region, and the bottom (*gray*) stratum represents the tails. The yellow spheres denote Ca^{2+} ions that coordinate a ternary complex between PS and the central pocket. (*a*) The structure of the water-soluble domain of Tim3 was inferred from a crystallographic analysis (26) and its membrane-bound structure refined by a combination of molecular dynamics (MD) simulations and x-ray reflectivity data (Fig. S1). The two images are rotated 180° around the membrane normal. BC, CC′, and FG are three flexible loops that contact the membrane. Two loops bear buried hydrophobic residues: W41 on the CC′ loop and L99 and M100 on the FG loop (*colored dark gray*). The red residues in the image on the left are the two arginine residues closest to the membranes, R50 and R54. The green residues in the image on the right are the two lysine residues proximal to the membrane, K103 and K104. Peripheral polar residues T25, S26, and S42 are colored yellow-orange. (*b*) The inferred docking of the water-soluble domain of Tim1 to the monolayer similarly refined from a combination of MD simulations and x-ray reflectivity, taken from Tietjen et al. (35). R25 and R53 are colored red, K102 is colored green, W97 and F98 are colored dark gray, and S40 is colored yellow-orange. (*c*) The inferred docking of the water-soluble domain of Tim4 (Protein Data Bank: 3BIB) to the monolayer, taken from Tietjen et al. (14). R27 and R48 are colored red, K41 and K102 are colored green, W97 and F98 are colored dark gray, and S40 is colored yellow-orange. Calcium was substituted for the sodium ion resolved in the crystal structure (15) as in Tietjen et al. (14). To see this figure in color, go online.

Membrane binding of the three Tim proteins

The Ig domain of Tim1 and Tim4 each has three tryptophan residues, whereas that of Tim3 only has two; when Tim1, Tim3, or Tim4 associates with the membrane, a single tryptophan side chain is buried (Fig. 1). We used the consequent shift in the tryptophan fluorescence emission spectra to monitor the association of the proteins with membranes composed of various mixtures of 1-palmitoyl-2-oleoyl-sn-glycero-3-phosphocholine (POPC) and 1-palmitoyl-2-oleoyl-sn-glycero-3-phospho-L-serine (POPS) (Fig. 2; see Supporting materials and methods for analysis details) (14,35,40). The differences among the observed fluorescence shifts of the three Tim proteins are likely due to the different environments of the inserted tryptophan of each Tim protein. In particular, the blue-shifts observed for the binding of Tim1 and Tim4 proteins were both 18 nm, whereas the blue-shift for Tim3 was 10 nm (Fig. 2). This result is consistent with shallower insertion of the tryptophan of Tim3, which is located on the superficial CC′ loop, as opposed to that of Tim1 and Tim4 on the FG loop (Fig. 1). Unlike Tim3, both Tim1 and Tim4 bound to membranes containing 7:3 mixtures of POPC and POPS in the absence of Ca^{2+}, albeit weakly (Fig. 2). Tim1 bound equally weakly to neat POPC vesicles in the absence of both POPS and Ca^{2+} (Fig. 2 *b*, *inset*). Neither Mg^{2+} nor Ba^{2+} supported the binding of any Tim protein to POPS-containing vesicles (data not shown).

Calcium dependence of binding

Using the same vesicle conditions as the experiments depicted in Fig. 2, the $[Ca^{2+}]$ dependence of the membrane association of the Tim proteins was determined (Fig. 3). These isotherms were hyperbolic, consistent with the involvement of a single Ca^{2+} in the binding interactions shown in Fig. 1. These curves fit well to a modified Michaelis-Menten model derived in the Supporting materials and methods and presented as Eq. 1.

$$\frac{b}{b_{tot}} = \frac{b_{max}}{b_{tot}} \frac{[Ca^{2+}]}{\mathrm{EC50} + [Ca^{2+}]} + \frac{b_0}{b_{tot}} \frac{\mathrm{EC50}}{\mathrm{EC50} + [Ca^{2+}]}. \quad (1)$$

Fig. 3 *a* spells out the meaning of these parameters: b is the bound fraction of protein as revealed by fluorescence. Protein that does not bind and protein that binds but does not have a fluorescent shift, do not affect our analysis. b_0 represents binding in the absence of Ca^{2+} and b_{max} represents binding at saturating $[Ca^{2+}]$ at a given {POPS}. Curly brackets denote the membrane concentration of a phospholipid in mol%. b_{tot} is full binding of the input protein when both $[Ca^{2+}]$ and {POPS} are saturated and is obtained empirically, i.e., it is not a fit parameter because it appears on both sides of Eq. 1 and thus its value cannot be determined by regression. EC50 (the half maximal effective concentration) is the Ca^{2+} concentration that produced half-maximal protein binding on the hyperbola between b_0 and b_{max} at a given {POPS}.

Fig. 3, *b–d* present binding isotherms for the three Tim proteins. They were analyzed using Eq. 1 to obtain values for the binding parameters (Table 1). Note that Tim1 and Tim4 associated with the membranes in the absence of Ca^{2+}, as also seen in Fig. 2. Importantly, the saturation of binding reached a plateau at $b_{max} < b_{tot}$ whenever the availability of PS was limiting. This is because of the {POPS} dependence of the b_{max} and the EC50 for calcium (see Eqs. S7 and S8 as well as the Discussion). In other words, despite its widespread usage, EC50-values are not true dissociation constants for the binding of proteins like Tim

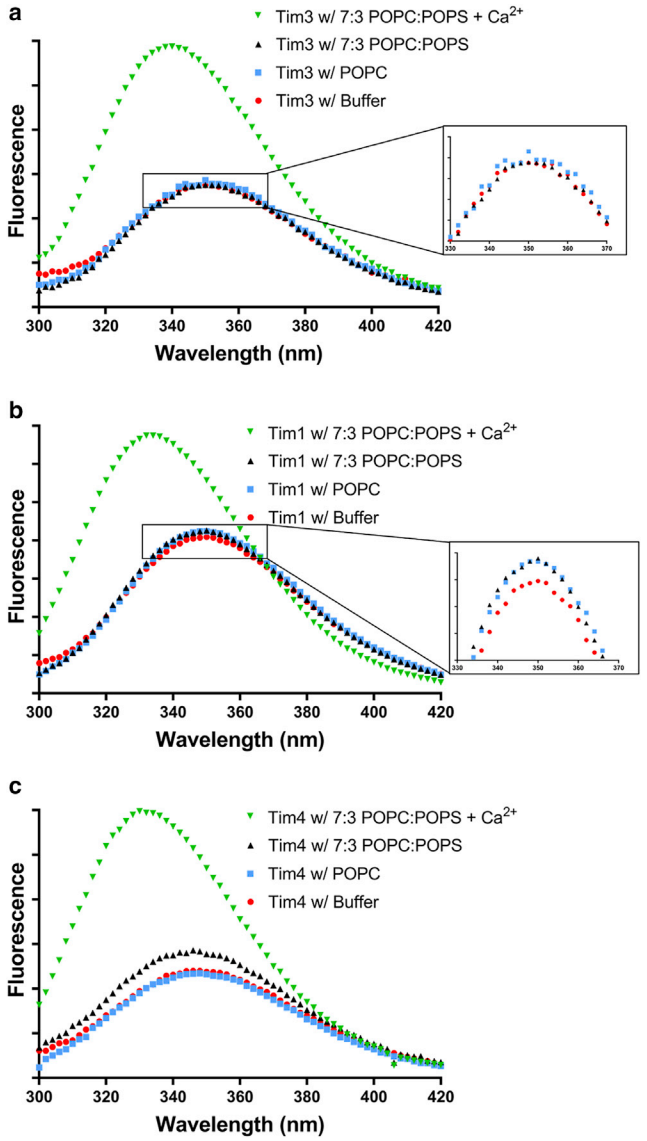

FIGURE 2 Tryptophan spectra of membrane-bound Tim proteins. Emission spectra of (*a*) Tim3, (*b*) Tim1, and (*c*) Tim4 were recorded without lipids or with 300 μM vesicles composed of POPC or 7:3 POPC/POPS in the presence and absence of these previously-determined saturating levels of calcium: 2 mM for Tim1, 8 mM for Tim3, and 0.6 mM for Tim4. The *y* axes represent arbitrary fluorescence units normalized for each Tim protein. The error bars are smaller than the data points. To see this figure in color, go online.

to either Ca^{2+} or to the bilayer. Nevertheless, we show below how EC50-values can be used as proxies for the membrane affinity of a Tim protein. (It is not meaningful to compare the EC50 values for the Tim proteins for a single membrane nor the differences in their EC50 values for different membranes. Nevertheless, EC50-values faithfully represent binding affinities for a given Tim protein under different membrane conditions. We therefore use EC50-values as a proxy for membrane affinity throughout this study. See Supporting materials and methods for more details.)

Effect of phospholipid unsaturation on Tim binding

Both the molecular models (Fig. 1) and the blue-shift in the tryptophan fluorescence spectra (Fig. 2) suggested that the membrane association of Tim proteins involved hydrophobic interactions. In that case, weakening the packing and cohesion of the bilayer phospholipids should strengthen Tim binding by increasing its accommodation (41–43). We, therefore, determined the binding of the Tim proteins to bilayers composed of phospholipids with increasing unsaturation. Substituting 1,2-dioleoyl (DO) lipids for PO lipids caused a roughly threefold decrease in the EC50 and a commensurate increase in the b_0 and b_{max} of all three Tim proteins (Fig. 3, *b–d*; Table 1). Furthermore, the EC50 for Tim3 decreased linearly with the abundance of the DO phospholipid in the vesicles (Fig. 3 *e*). The higher b_0-values for Tim1 and Tim4 than for Tim3 are consistent with their greater calcium-independent interaction with the membranes seen in Fig. 2.

A mathematical model for the binding reaction

We next determined the effect of {POPS} on the binding of the Tim proteins at varied $[Ca^{2+}]$ (Fig. 4). As mentioned above, EC50 is a useful metric for gauging the dependence of protein binding on $[Ca^{2+}]$ at a fixed {POPS} but it does not capture the complex interplay between Ca^{2+} and PS. We therefore constructed an expression that not only embraces the co-dependence of binding on $[Ca^{2+}]$ and {POPS} but also on total lipid concentration [L]. It is presented here as Eq. 2 and as Eq. S1:

$$\frac{b}{b_{tot}} = \frac{\left(\frac{1}{K_{TS}} + \frac{[Ca^{2+}]}{K^2}\right)[L]\left(\frac{[PS]}{[L]}\right)^h}{1 + \frac{[Ca^{2+}]}{K_{TC}} + \left(\frac{1}{K_{TS}} + \frac{[Ca^{2+}]}{K^2}\right)[L]\left(\frac{[PS]}{[L]}\right)^h}. \quad (2)$$

K is the dissociation constant for the overall binding reaction involving Tim, Ca^{2+}, and the membrane. h resembles a Hill coefficient denoting cooperative dependence on {POPS}. K_{TC} is the dissociation constant for a membrane-free Tim-Ca^{2+} complex. K_{TS} embraces all interactions (e.g., electrostatic and hydrophobic) of a Tim protein with the membrane other than the Tim-Ca^{2+}-PS linkage. Each dissociation constant is expressed in units of micromolar. Unlike K_{TC}, the dissociation constants for K and K_{TS} cannot be compared among the Tim proteins because the moieties engaged in the binding reactions differ, thus imparting different reaction orders. These are reflected in their h-values; see Discussion and (44). b_{tot} is, again, full binding of the input protein when $[Ca^{2+}]$ and {POPS} are saturating but now is a parameter determined through fitting. Note that the model does not explicitly incorporate hydrophobic effects or bilayer lipid packing.

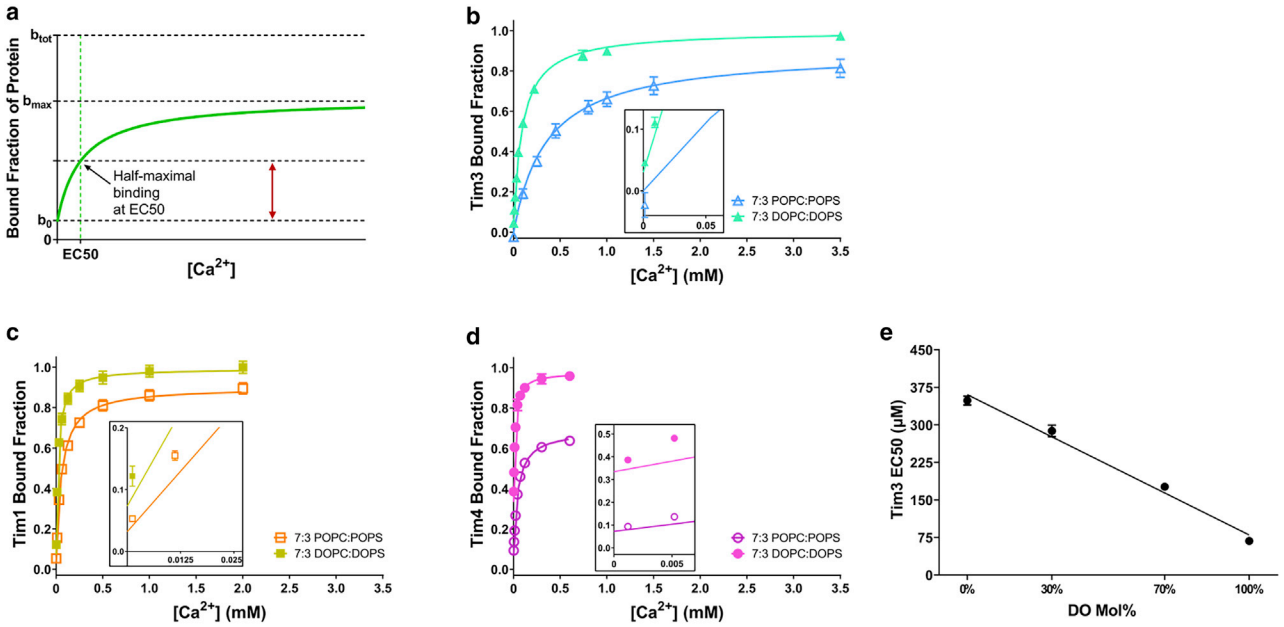

FIGURE 3 Ca^{2+} dependence of Tim protein binding to bilayers composed of two different phospholipids. (*a*) Graphical definitions of the parameters for Tim protein binding in a Ca^{2+}-dependent isotherm (see text). Binding curves for (*b*) Tim3, (*c*) Tim1, and (*d*) Tim4 were obtained with vesicles of 300 μM phospholipid composed of 70 mol% POPC plus 30 mol% POPS or 70 mol% 1,2-dioleoyl-sn-glycero-3-phosphocholine (DOPC) plus 30 mol% 1,2-dioleoyl-sn-glycero-3-phospho-L-serine (DOPS). Best fit curves were generated by nonlinear least squares using Eq. 1. Insets: Blowup of the *y* axis intercepts. (*e*) Effect of diunsaturated DO phospholipids on the EC50 of Tim3. The descending data points correspond to the use of 7:3 mixtures of POPC/POPS, POPC/DOPS, DOPC/POPS, and DOPC/DOPS, with DO mol% of 0, 30, 70, and 100%, respectively. The data were obtained as in (*c*). The error bars for all plotted data represent standard errors, most of which are smaller than the data points. To see this figure in color, go online.

Interplay between PS and Ca^{2+} in Tim binding

The Ca^{2+} dependent binding of Tim proteins to bilayer PS is pictured in Fig. 4 *a*. Experimental results for the Tim3 reaction are shown in Fig. 4 *b* and replotted in Fig. 4 *c*. Fig. 4 *b* shows a hyperbolic (first-order) $[Ca^{2+}]$ dependence for Tim3 binding at all {POPS}. The sigmoidal shape of the replotted data in Fig. 4 *c* suggests a higher order concentration dependence on {POPS}, cooperative binding, at every calcium concentration. This cooperativity is reflected in the value of the Hill coefficient for Tim3 obtained here, 1.65 $\pm$ 0.07, and is consistent with the value we previously measured, 1.9 $\pm$ 0.5 (14). (The previously obtained value for the Hill coefficient of Tim3 was recalculated after reanalysis of the primary data using the updated data analysis methodology of this work; see Supporting materials and methods.)

TABLE 1 Values for Tim protein binding to vesicles composed of PO and DO phospholipids

Binding parameter	Tim1	Tim3	Tim4
EC50 for PO lipids, μM	57 (48, 66)	355 (277, 432)	45 (40, 51)
EC50 for DO lipids, μM	22 (19, 24)	92 (85, 100)	16 (14, 18)
b_0 for PO lipids	0.03 (0.02, 0.05)	0 (0, 0.03)	0.07 (0.06, 0.08)
b_0 for DO lipids	0.07 (0.05, 0.1)	0.03 (0.02, 0.04)	0.33 (0.31, 0.35)
b_{max} for PO lipids	0.90 (0.85, 0.95)	0.90 (0.85, 0.96)	0.69 (0.67, 0.71)
b_{max} for DO lipids	0.99 (0.97, 1.00)	1.00 (0.99, 1.00)	0.98 (0.96, 1.00)

Values were obtained by fitting data in Fig. 3, *b–d* to Eq. 1. Briefly, the vesicles contained 7:3 PC/PS, the fatty acyl chains of which were either PO or DO and total lipid concentration was 300 μM. Brackets give 95% confidence intervals. The values for each parameter are significantly different for the three Tim proteins at >95% confidence as calculated using a *z* test.

Curves fitting the data in Fig. 4, *b and c* were obtained in two ways with effectively equivalent results. Eq. 1 directly delivers a useful parameter, EC50, from a three-parameter fit to each data set in Fig. 4 *b*. These values were plotted in Fig. 4 *d*. More powerfully, Eq. 2 yielded a single set of values, given in Table 2, that generated "all" of the curves in Fig. 4, *b and c*. The dependence of EC50 on {POPS} was then calculated from the values in Table 2 using Eq. S7 and the results used to generate the curve shown in Fig. 4 *d*. The relative utility of Eq. 1 is that it is less dependent on the assumptions underlying Eq. 2. However, the match of the EC50 curve obtained from the analysis using Eq. 2 to the corresponding values from Eq. 1 speaks to the validity of the mathematical model.

Data for the dependence of Tim1 and Tim4 binding on $[Ca^{2+}]$ and on total lipid concentration [L] at fixed {POPS} are shown in Figs. S3 and S4. Using the values for the Hill coefficients previously determined from experiments with fixed [L] and varying {POPS} (14), Eq. 2 was fit to these data and yielded the values for the dissociation constants given in Table 2. These were used with Eq. S7 (derived from Eq. 2) to generate the corresponding curves

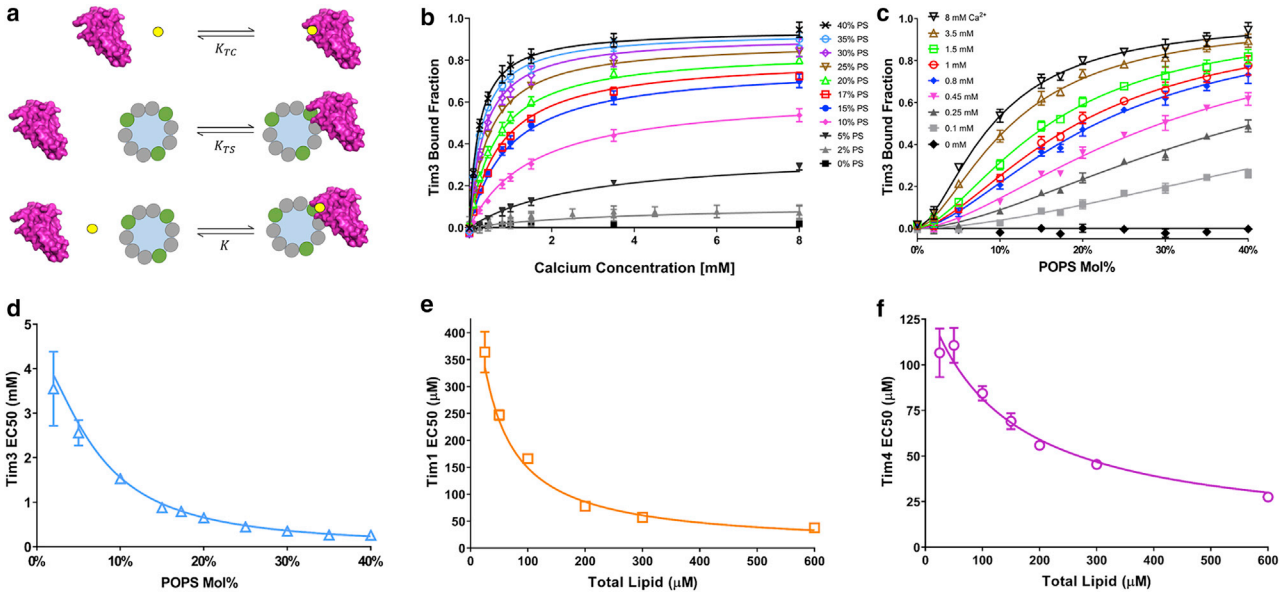

FIGURE 4 Dependence of Tim binding on [Ca^{2+}], {POPS}, and [total lipid]. (*a*) An illustration depicting formation of the tertiary complex. The protein is pink and the calcium ion is yellow; the green and gray circles represent PS and PC, respectively. (*b*) [Ca^{2+}] dependence of Tim3 binding to 300 μM POPC vesicles containing varied {POPS}. (*c*) The data in (*b*) were replotted as a function of {POPS}. The experimental values in (*b*) and (*c*) were fit to Eq. 2 to generate the curves. The values obtained are given in Table 2. (*d*) EC50-values were calculated from the data in (*b*) using Eq. 1. A curve matching these points was generated using the binding parameters for Tim3 in Table 2 and Eq. S7. (*e*) and (*f*) A multistep procedure was used to calculate the lipid concentration dependence of the binding of Tim1 and Tim 4. We applied the data in Figs. S3 and S4 to Eq. 1 to obtain the plotted EC50-values. As in (*d*), matching curves were generated using Eq. S7 and the values for the binding parameters in Table 2. Error bars (mostly hidden by data points) represent standard errors. To see this figure in color, go online.

in Fig. 4, *e and f*. As before, the fits of the curves to the data for Tim1 and Tim4 indicate the relevance and explanatory power of the model.

Interplay of additional anionic phospholipids with PS in Tim binding

The scrambling of the plasma bilayer allows all of the phospholipids normally sequestered in the cytoplasmic leaflet to equilibrate with the outer leaflet of the bilayer (see Introduction). We, therefore, examined the effect of varied 1-palmitoyl-2-oleoyl-sn-glycero-3-phosphate (POPA) and 1-palmitoyl-2-oleoyl-sn-glycero-3-phospho-(1'-rac-glycerol) (POPG) on Tim binding to vesicles with a total anionic phospholipid brought to 30 mol% with POPS (Fig. S6). The [Ca^{2+}] dependence of the binding of each Tim to each lipid mixture was invariably hyperbolic, validating the use of EC50 to describe the influence of these additional anionic lipids (Fig. 5). Strikingly, small amounts of POPA reduced the EC50 of Tim3 binding by a factor of 2.5 and reduced the EC50 of Tim4 binding by a factor of 1.5, but did not reduce the EC50 of Tim1. These reductions in EC50 correspond to an increase of the fractional binding of Tim3 from 0.67 to 0.81 (Fig. S6 *c*) and of Tim4 from 0.65 to 0.77 (both at 1 mM [Ca^{2+}]) (Fig. S6 *e*). In contrast to POPA, the similarly anionic POPG enhanced Tim3 association only mildly and did not enhance Tim4 association at all (Fig. 5, *a and c*). Whereas POPA was a more potent ligand than POPS, POPG seems to have merely substituted for POPS.

We also found that at {POPS} less than ~10 mol%, the binding of Tim proteins to POPG and POPA vesicles was

TABLE 2 Values for the parameters describing Tim protein binding to PS-containing vesicles

Binding parameter	Tim1	Tim3	Tim4
Hill coefficient, *h*	1.38 (1.2, 1.57)*	1.65 (1.59, 1.72)	2.28 (2.17, 2.39)*
K for Tim-Ca^{2+}-PS dissociation, μM	61 (59, 63)	127 (120, 136)	35 (34, 36)
K_{TC} for Tim-Ca^{2+} dissociation, μM	590 (540, 650)	4300 (3600, 5200)	136 (123, 150)
K_{TS} for Tim-PS dissociation, μM	1800 (1300, 2700)	>5000	239 (220, 258)

Values for Tim3 were obtained by fitting the data in Fig. 4, *b and c* to Eq. S4. Values for Tim1 and Tim4 were obtained by fitting the data in Figs. S3 and S4 to Eq. 2, utilizing *h*-values recalculated from the primary data for Figure 5 of Tietjen et al. (14). Brackets give 95% confidence intervals. The values for each parameter are significantly different for the three Tim proteins at >95% confidence as calculated using a *z* test.

*The previously obtained values for the Hill coefficients of Tim1 and Tim4 were recalculated after reanalysis of the primary data using the updated data analysis methodology of this work; see Supporting materials and methods.

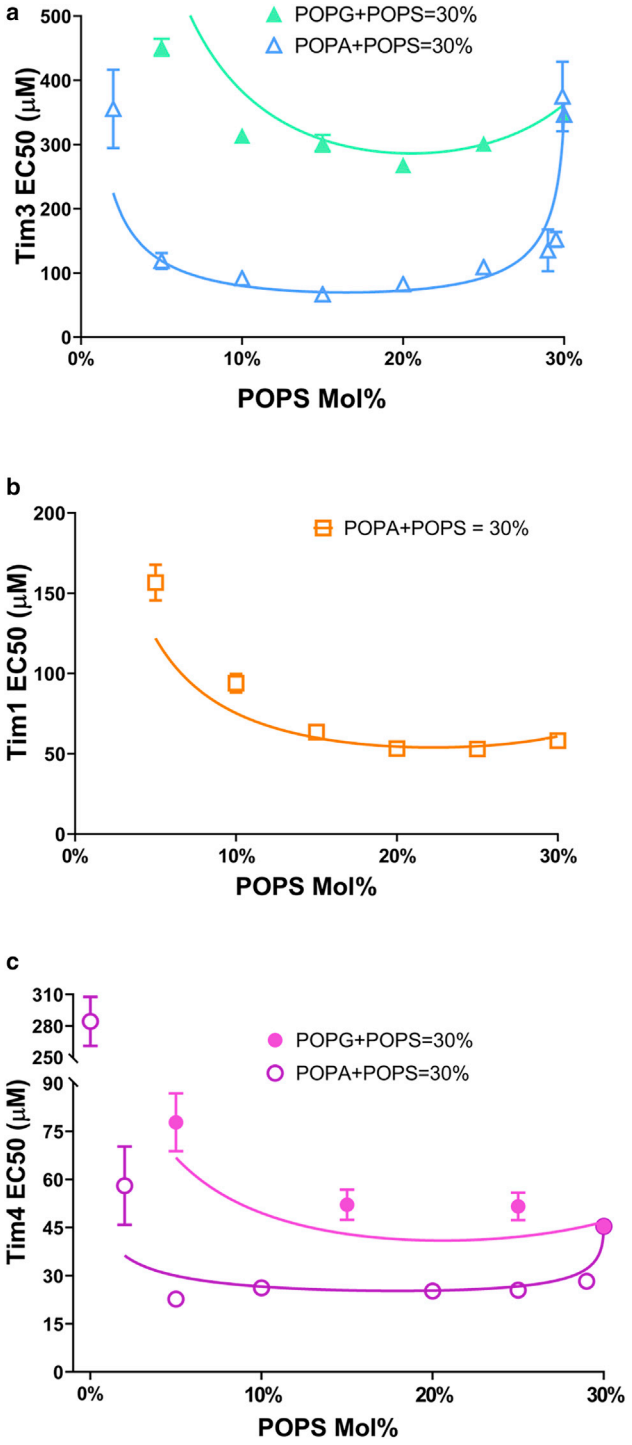

FIGURE 5 Effect of POPA and POPG on the binding of Tim proteins to POPC/POPS vesicles. The [Ca^{2+}] dependence of Tim protein binding was determined with 300 μM vesicles composed of 70 mol% POPC plus 30 mol % anionic phospholipids, distributed between POPS and POPA or between POPS and POPG. The primary data are shown in Fig. S6. Theoretical curves were generated by fitting the values listed in Table S2 to Eq. S12. Error bars (mostly hidden by the data points) represent standard errors. (*a*) Tim3, (*b*) Tim1, and (*c*) Tim4. To see this figure in color, go online.

weak. Presumably, this is because the crucial linkage, Tim-Ca^{2+}-PS, was diminished. At {POPS} greater than 10 mol %, {POPA} had little or no effect on the observed [Ca^{2+}] dependence of Tim1. Membranes lacking POPS bound Tim4 weakly (Figs. 5 *c* and S6 *e*) but Tim1 and Tim3 gave no observable binding (data not shown). Thus, POPA and POPG did not simply substitute for POPS; presumably, a higher order interaction is involved. That the binding of Tim3 and Tim4 is significantly enhanced by small amounts of POPA in POPS-containing membranes but not much by POPA in the absence of POPS suggests synergism between POPA and POPS, pointing to heterotropic cooperativity. This is borne out in the values for the binding parameters (Table S2). A detailed consideration of these relationships is considered in the Supporting materials and methods; in particular see Eq. S12.

DISCUSSION

The modeling of the dispositions of the Tim proteins shown in Fig. 1 suggests that their binding depends on the interplay of at least these four factors: 1) calcium coordination with PS; 2) hydrophobic contacts; 3) bilayer packing that resists the burial of hydrophobic side chains; and 4) electrostatic interactions with anionic phospholipids, predominantly PS and PA. The biochemical tests employed in this study explored these hypotheses, and the resulting data, when analyzed using the mathematical model described above, provide insights into the complex interactions.

Because the experiments of Figs. 4 and 5 sampled a wide range of POPS and POPA compositions, the binding parameters obtained therefrom allow extrapolation to other compositions. We considered conditions relevant to activated and/or apoptotic cells; namely, 1 mM Ca^{2+}, 10 mol% POPS, and 1 mol% POPA (29,30,33,45–49). Our findings are summarized in Fig. 6, generated using Eq. S12 and the experimental values depicted in Figs. 4 and 5. Fig. 6 *a* charts the dependence of Tim binding on POPA and the importance of calcium; Fig. 6 *b* charts the dependence of Tim binding on POPS under the influence of POPA. That the proteins did not bind appreciably to bilayers lacking anionic phospholipids is in accord with their sparing of quiescent cells in vivo. As seen in Fig. 6 *a*, the binding of Tim3 (*blue curve*) and Tim4 (*magenta curve*) increases greatly with {POPA} up to 1 mol%. Above this threshold, their binding flattens to match the {POPA} dependence of Tim1 (*orange curve*) at a subsaturating level.

Fig. 6 *b* illustrates that, in the absence of POPA, the sigmoidicity in the binding of the Tim proteins to POPS differs according to their Hill coefficients (Table 2). POPA reduced the cooperativity of Tim3 and Tim4 binding to POPS, as seen in the change in the shape of the binding curves from sigmoidal to nearly hyperbolic (*blue and purple dotted to solid curves*). POPA also significantly bolstered their affinity for POPS-containing membrane to exceed that of Tim1. The enhancement in binding and the reduction of

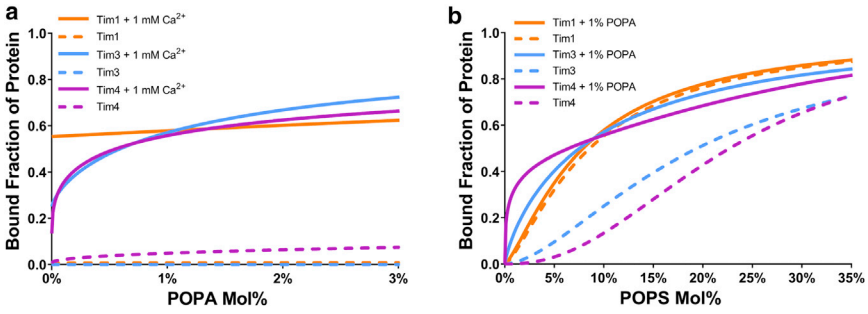

FIGURE 6 Calculated membrane binding of Tim proteins. Curves were generated with Eq. S12 using the values in Tables 2 and S2 and a total lipid of [L] = 300 μM. This is approximately the level of phospholipid available in plasma membranes in a 10% v/v cell suspension. (*a*) Protein binding at {POPS} = 10 mol% as a function of {POPA} with or without 1 mM [Ca^{2+}]. (*b*) Protein binding at [Ca^{2+}] = 1 mM as a function of {POPS} with or without 1 mol% {POPA}. To see this figure in color, go online.

cooperativity by 1 mol% POPA suggest that POPA substitutes for POPS in interactions peripheral to the Tim-Ca^{2+}-PS linkage in the central pocket. Furthermore, the hyperbolic dependence of Tim3 and Tim4 on POPA seen in Fig. 6 *a* indicates that the interaction with POPA is predominantly first order; i.e., the association of the protein with a single POPA is sufficient to impart increased sensitivity to POPS (see Supporting materials and methods; Table S2).

Interestingly, in the presence of 1 mol% POPA, the binding curves for the three Tim proteins intersect at ~10 mol% POPS and closely overlap above this value (Fig. 6 *b*). The value for this intersection point depends on {POPA} and [Ca^{2+}], but not [L] (see Eq. S12). Taken together, Fig. 6 demonstrates that 1 mM Ca^{2+}, 10 mol% POPS, and 1 mol % POPA define a region of convergence for the binding of the three Tim proteins, outside of which their binding diverges. Because these conditions are relevant to those for apoptotic membranes, they suggest that, although the mechanisms driving Tim1, Tim3, and Tim4 binding differ biophysically, they are nevertheless tuned to function similarly as membrane sensors for apoptosis.

The biochemical basis for the behavior of the Tim proteins illustrated in Fig. 6 is considered below.

Tim-Ca^{2+}-PS complexes

The central pockets of the three Tim proteins deploy polar and charged side chains that coordinate with bilayer PS through a calcium link. Neighboring nonpolar side chains also associate with the central pocket through van der Waals interactions (Fig. 1). Ca^{2+} must displace these side chains to bind (15,26). This competition reduces the calcium affinity of the proteins, especially Tim3. This is shown for K_{TC} in Table 2. On the other hand, the displacement of the apolar side chains by calcium would promote their contribution to membrane binding as reflected in the values for K in Table 2.

Hydrophobic associations

Our analysis did not quantify the contribution of the hydrophobic effect to Tim binding. However, that component was ever-present, given that the very detection of binding utilized the shift in fluorescence of their buried tryptophan side chains (Figs. 2 and 3). The importance of the nonpolar side chains was also shown by the reduction of the binding of the three proteins when those residues were deleted (15,26). It was presumably those nonpolar contacts that promoted Tim1 binding in the absence of Ca^{2+} and PS (Fig. 2). That Tim3 interacts hydrophobically with the bilayer was also evinced by the inhibitory effect of 2 M urea (Fig. S2). This chaotrope would promote the partition of its hydrophobic side chains to the aqueous phase and thereby reduce their transfer to the bilayer, as seen, for example, in the inhibitory effect of urea on the binding of annexin V to membranes (50).

Membrane accommodation

The insertion of Tim proteins into the bilayer works against the elastic cohesion of the phospholipids. Unsaturated phospholipid tails pack more loosely than their saturated counterparts and thus, better accommodate protein insertion (49,51). This is presumably why substituting diunsaturated for monounsaturated phospholipids enhanced the binding of all three Tim proteins (Fig. 3; Table 1). Furthermore, vesicles containing the more condensed dimyristoylphosphatidylserine with its saturated tails allowed no detectable binding of Tim3 (data not shown). Other peripheral proteins show similar behavior (41,42).

These observations have functional relevance. Phospholipids with unsaturated fatty acyl chains are enriched in the cytoplasmic leaflets of plasma membrane and move to the surface of triggered (e.g., apoptotic) cells (29,49,52–54). Furthermore, plasma membrane phospholipids become more unsaturated in triggered lymphocytes (55–57). These effects would favor the accommodation of Tim proteins.

Electrostatic interactions

A variety of peripheral proteins interact electrostatically with anionic phospholipids (1–3,34,58–60). In the case of Tim proteins, the multiple basic side chains adjacent to the central pocket bind bilayer PS (Fig. 1) (14,26,35,61). The sigmoidal dependence of Tim4 binding on bilayer POPS concentration is taken to reflect contributions by its two lysine and two arginine side chains in addition to its

ternary calcium link (Fig. 6 *b*; Table 2). This inference is supported by mutational studies: removal of these residues reduces the cooperativity of Tim4 binding to POPS (14). This behavior does not reflect allosteric conformational transitions but rather the concerted free energies of association of each of the multiple ligands, amplified by the reduction of dimensionality arising from membrane binding (4,43,62). That the basic side chains in Tim3 do not abut the anionic PS headgroups as closely as those of Tim4 can account for the lower cooperativity of its binding (Figs. 1 *a* and 4 *b*; Table 2; (14,26)). Similarly, the shallow sigmoidicity of Tim1 binding is consistent with the disposition of its single lysine and arginine residues (Fig. 1 *b*; (35)).

The effect of an additional anionic phospholipid

Membranes containing only POPA or POPG in place of POPS bound Tim proteins weakly at best, even in the presence of calcium (data not shown for Tim1 and Tim3 but, for Tim4, see Fig. 5 *c* at 0% POPA and POPG). On the other hand, POPA strongly promoted the binding of Tim3 and Tim 4 to POPS-containing bilayers (Figs. 5, *b and c* and 6). The strong effect of traces of POPA on the binding of Tim3 and Tim4 suggests a direct interaction with these proteins.

That PA is a potent ligand for two Tim proteins is explained by its molecular features (Fig. 5; Table S2) (63,64). At pH 7.5, its diacidic headgroup has a negative charge of ~1.5 (65–68). The basic side chains on a bound protein can bring its charge close to –2 (65). Variations of ambient pH could, therefore, affect Tim binding in vivo. PA has a conical contour and a small headgroup that lies close to the nonpolar stratum. Both of these features would promote protein association with the bilayer. In addition, the polar heads of PA and PG lack the positive charge found on PS that could interfere with electrostatic interactions with the cationic side chains. Note that POPG has the same unitary net negative charge and nearly the same cross section as POPS, yet it differs dramatically in its interaction with the Tim proteins (Fig. 5, *b and c*) (69,70). We conclude that the interactions of Tim proteins with the varied anionic headgroups differ according to 1) their ability to form a Ca^{2+} coordination complex; 2) their electrostatic interactions with basic side chains; 3) their molecular geometry; and 4) their intimate stereochemical association with the membrane contact surface of the proteins.

A role for cell surface PA in intercellular signaling

PA was proposed as a cell surface signal decades ago (71,72). Much subsequent evidence supports this hypothesis. The pool of PA in triggered thymocytes can change on a timescale of minutes (73). A wide variety of physiological, pathological, and immune processes involve an increase in plasma membrane PA through the activation of phosphatidylcholine phospholipase D (PC-PLD) (71,74–76). Notably, cell activation causes the transfer of PC-PLD from the cytoplasm to the inner leaflet of the plasma membrane (77,78). The PA produced there can be translocated to the cell surface by the same nonspecific scramblase that exposes PS (29,33). Outer leaflet PA can itself activate scramblase, intensifying responses (79). Cell surface PA then modulates several downstream pathways (28,80).

Similarly, in acute inflammation, the apoptosis of neutrophils after they ingest foreign particles is promoted by the PA produced by their PC-PLD (81–84). In a highly regenerative process, the nascent PA can intensify its own elaboration by activating PC-PLD (75). Calcium-triggered scrambling would bring this PA as well as PS to the cell surface. The surface exposure of these anionic phospholipids would promote the removal of apoptotic neutrophils by phagocytes bearing Tim proteins.

CONCLUSIONS

We have shown that the association of Tim1, Tim3, and Tim4 with synthetic phospholipid vesicles is sensitive to conditions likely to obtain for apoptotic and other triggered cells in vivo. That is, the binding of each was responsive to a different degree to calcium, PS, PA, and bilayer unsaturation (Fig. 6). The membranes act as multidentate chelators of the Tim proteins, and this multiplicity of effectors, acting through positive and negative cooperative interactions, tunes the strength as well as the selectivity of protein binding. Tim1 bound strongly through hydrophobic associations rather than electrostatic forces (Figs. 2 and 3) as revealed by the small exponent for its binding to {POPS} (*h* in Table 2) and its poor response to POPA (Figs. 5 *a* and 6 *a*). The influence of electrostatic interactions for Tim3 was clear from the cooperativity of its POPS dependence and its response to POPA (Figs. 5 *b* and 6 *a*). A hydrophobic effect for Tim3 was surmised from the inhibition of its binding by urea (Fig. S2). Finally, Tim4 binding was strongly promoted by Ca^{2+} (Fig. 3), hydrophobic interactions (Figs. 2 and 3) and multiple electrostatic interactions, as reflected in the sigmoidicity of its POPS isotherm (Table 2) and its response to POPA (Figs. 5 *c* and 6 *a*).

These results provide insight into how the Tim proteins and perhaps other PS receptors deployed on the surfaces of different immune surveillance cells not only specifically recognize PS-presenting target cells but differentiate among them. In particular, the varied sensitivity of these proteins to the combined influences of lipid unsaturation, calcium, and PA modulates their affinity for PS-bearing membranes. Tim1 is rather indifferent to these auxiliary attributes and is thus less responsive to the membrane context other than its recognition of PS. In contrast, Tim3 and Tim4 respond to several features of apoptotic cell surfaces. That our mathematical model provides satisfying insights into the complex bilayer interactions of Tim3 suggests its explanatory

potential for other peripheral membrane proteins. Finally, the nuanced selectivity of the Tim proteins described herein highlights the importance of target membrane context for the function of membrane-binding proteins.

SUPPORTING MATERIAL

Supporting material can be found online at https://doi.org/10.1016/j.bpj.2021.09.016.

AUTHOR CONTRIBUTIONS

D.K., Z.G., G.T.T., E.J.A., and K.Y.C.L. designed research. D.K., Z.G., T.S., G.T.T., A.L., S.R., R.S., H.L.H., J.M.H., and K.D.C. performed research. W.B. and B.L. contributed new reagents/analytic tools. D.K., Z.G., W.B., and B.L. analyzed data. D.K., Z.G., G.T.T., T.L.S., E.J.A., and K.Y.C.L. wrote the paper.

ACKNOWLEDGMENTS

We thank Elena Solomaha, Nathaniel Posner, and Yvonne Lange for their input into this study.

This work was supported by the National Science Foundation through MCB-1950525 (to K.Y.C.L.). K.Y.C.L. acknowledges support from The University of Chicago Materials Research Science and Engineering Center (DMR-2011854) and The University of Chicago Biophysics Core Facility. National Science Foundation's ChemMatCARS Sector 15-ID is principally supported by the National Science Foundation under Grant NSF/CHE-1834750. Additional National Institutes of Health support was provided under grants No. R01-GM101048, U54-GM087519, and P41-GM104601 (to E.J.A.). D.K. acknowledges the support of the National Institutes of Health Molecular and Cell Biology training grant (T32 GM007183). Use of the Advanced Photon Source was supported by the DOE Office of Science, Office of Basic Energy Sciences, under Contract DE-AC02-06CH11357.

REFERENCES

1. Whited, A. M., and A. Johs. 2015. The interactions of peripheral membrane proteins with biological membranes. *Chem. Phys. Lipids.* 192:51–59.
2. Heimburg, T., B. Angerstein, and D. Marsh. 1999. Binding of peripheral proteins to mixed lipid membranes: effect of lipid demixing upon binding. *Biophys. J.* 76:2575–2586.
3. Kinnunen, P. K., A. Kõiv, …, P. Mustonen. 1994. Lipid dynamics and peripheral interactions of proteins with membrane surfaces. *Chem. Phys. Lipids.* 73:181–207.
4. Denisov, I. G., and S. G. Sligar. 2012. A novel type of allosteric regulation: functional cooperativity in monomeric proteins. *Arch. Biochem. Biophys.* 519:91–102.
5. Freeman, G. J., J. M. Casasnovas, …, R. H. DeKruyff. 2010. TIM genes: a family of cell surface phosphatidylserine receptors that regulate innate and adaptive immunity. *Immunol. Rev.* 235:172–189.
6. Anderson, A. C., N. Joller, and V. K. Kuchroo. 2016. Lag-3, Tim-3, and TIGIT: co-inhibitory receptors with specialized functions in immune regulation. *Immunity.* 44:989–1004.
7. Ocaña-Guzman, R., L. Torre-Bouscoulet, and I. Sada-Ovalle. 2016. TIM-3 regulates distinct functions in macrophages. *Front. Immunol.* 7:229.
8. Angiari, S., and G. Constantin. 2014. Regulation of T cell trafficking by the T cell immunoglobulin and mucin domain 1 glycoprotein. *Trends Mol. Med.* 20:675–684.
9. Flannagan, R. S., J. Canton, …, S. Grinstein. 2014. The phosphatidylserine receptor TIM4 utilizes integrins as coreceptors to effect phagocytosis. *Mol. Biol. Cell.* 25:1511–1522.
10. Clayton, K. L., M. B. Douglas-Vail, …, M. A. Ostrowski. 2015. Soluble T cell immunoglobulin mucin domain 3 is shed from CD8+ T cells by the sheddase ADAM10, is increased in plasma during untreated HIV infection, and correlates with HIV disease progression. *J. Virol.* 89:3723–3736.
11. Schweigert, O., C. Dewitz, …, J. Scheller. 2014. Soluble T cell immunoglobulin and mucin domain (TIM)-1 and -4 generated by A Disintegrin And Metalloprotease (ADAM)-10 and -17 bind to phosphatidylserine. *Biochim. Biophys. Acta.* 1843:275–287.
12. Kobayashi, N., P. Karisola, …, G. J. Freeman. 2007. TIM-1 and TIM-4 glycoproteins bind phosphatidylserine and mediate uptake of apoptotic cells. *Immunity.* 27:927–940.
13. Nakayama, M., H. Akiba, …, K. Okumura. 2009. Tim-3 mediates phagocytosis of apoptotic cells and cross-presentation. *Blood.* 113:3821–3830.
14. Tietjen, G. T., Z. Gong, …, E. J. Adams. 2014. Molecular mechanism for differential recognition of membrane phosphatidylserine by the immune regulatory receptor Tim4. *Proc. Natl. Acad. Sci. USA.* 111:E1463–E1472.
15. Santiago, C., A. Ballesteros, …, J. M. Casasnovas. 2007. Structures of T cell immunoglobulin mucin protein 4 show a metal-Ion-dependent ligand binding site where phosphatidylserine binds. *Immunity.* 27:941–951.
16. McGrath, M. M. 2018. Diverse roles of TIM4 in immune activation: implications for alloimmunity. *Curr. Opin. Organ Transplant.* 23:44–50.
17. De Sousa Linhares, A., F. Kellner, …, P. Steinberger. 2020. TIM-3 and CEACAM1 do not interact in cis and in trans. *Eur. J. Immunol.* 50:1126–1141.
18. Leitner, J., A. Rieger, …, P. Steinberger. 2013. TIM-3 does not act as a receptor for galectin-9. *PLoS Pathog.* 9:e1003253.
19. Zhu, C., A. C. Anderson, …, V. K. Kuchroo. 2005. The Tim-3 ligand galectin-9 negatively regulates T helper type 1 immunity. *Nat. Immunol.* 6:1245–1252.
20. Kikushige, Y., T. Miyamoto, …, K. Akashi. 2015. A TIM-3/Gal-9 autocrine stimulatory loop drives self-renewal of human myeloid leukemia stem cells and leukemic progression. *Cell Stem Cell.* 17:341–352.
21. Wilker, P. R., J. R. Sedy, …, K. M. Murphy. 2007. Evidence for carbohydrate recognition and homotypic and heterotypic binding by the TIM family. *Int. Immunol.* 19:763–773.
22. Chiba, S., M. Baghdadi, …, M. Jinushi. 2012. Tumor-infiltrating DCs suppress nucleic acid-mediated innate immune responses through interactions between the receptor TIM-3 and the alarmin HMGB1. *Nat. Immunol.* 13:832–842.
23. Huang, Y. H., C. Zhu, …, R. S. Blumberg. 2015. CEACAM1 regulates TIM-3-mediated tolerance and exhaustion. *Nature.* 517:386–390.
24. Naeini, M. B., V. Bianconi, …, A. Sahebkar. 2020. The role of phosphatidylserine recognition receptors in multiple biological functions. *Cell. Mol. Biol. Lett.* 25:23.
25. Cao, E., X. Zang, …, S. C. Almo. 2007. T cell immunoglobulin mucin-3 crystal structure reveals a galectin-9-independent ligand-binding surface. *Immunity.* 26:311–321.
26. DeKruyff, R. H., X. Bu, …, J. M. Casasnovas. 2010. T cell/transmembrane, Ig, and mucin-3 allelic variants differentially recognize phosphatidylserine and mediate phagocytosis of apoptotic cells. *J. Immunol.* 184:1918–1930.
27. Santiago, C., A. Ballesteros, …, J. M. Casasnovas. 2007. Structures of T Cell immunoglobulin mucin receptors 1 and 2 reveal mechanisms for regulation of immune responses by the TIM receptor family. *Immunity.* 26:299–310.
28. Stace, C. L., and N. T. Ktistakis. 2006. Phosphatidic acid- and phosphatidylserine-binding proteins. *Biochim. Biophys. Acta.* 1761:913–926.

29. Bevers, E. M., and P. L. Williamson. 2016. Getting to the outer leaflet: physiology of phosphatidylserine exposure at the plasma membrane. *Physiol. Rev.* 96:605–645.

30. Murate, M., and T. Kobayashi. 2016. Revisiting transbilayer distribution of lipids in the plasma membrane. *Chem. Phys. Lipids.* 194:58–71.

31. Segawa, K., J. Suzuki, and S. Nagata. 2011. Constitutive exposure of phosphatidylserine on viable cells. *Proc. Natl. Acad. Sci. USA.* 108:19246–19251.

32. Rysavy, N. M., L. M. Shimoda, …, E. Y. Umemoto. 2014. Beyond apoptosis: the mechanism and function of phosphatidylserine asymmetry in the membrane of activating mast cells. *Bioarchitecture.* 4:127–137.

33. Williamson, P., A. Christie, …, E. M. Bevers. 2001. Phospholipid scramblase activation pathways in lymphocytes. *Biochemistry.* 40:8065–8072.

34. Tanguy, E., N. Kassas, and N. Vitale. 2018. Protein-phospholipid interaction motifs: a focus on phosphatidic acid. *Biomolecules.* 8:20.

35. Tietjen, G. T., J. L. Baylon, …, K. Y. C. Lee. 2017. Coupling X-ray reflectivity and in silico binding to yield dynamics of membrane recognition by Tim1. *Biophys. J.* 113:1505–1519.

36. Kerr, D. H. S. 2019. The membrane context of phosphatidylserine exposure influences its recognition by the TIM proteins: a structurally guided study. The University of Chicago, Dissertation https://knowledge.uchicago.edu/record/1993.

37. Sabatos-Peyton, C. A., J. Nevin, …, A. C. Anderson. 2017. Blockade of Tim-3 binding to phosphatidylserine and CEACAM1 is a shared feature of anti-Tim-3 antibodies that have functional efficacy. *OncoImmunology.* 7:e1385690.

38. Scharf, L., N. S. Li, …, E. J. Adams. 2010. The 2.5 Å structure of CD1c in complex with a mycobacterial lipid reveals an open groove ideally suited for diverse antigen presentation. *Immunity.* 33:853–862.

39. MacDonald, R. C., R. I. MacDonald, …, L. R. Hu. 1991. Small-volume extrusion apparatus for preparation of large, unilamellar vesicles. *Biochim. Biophys. Acta.* 1061:297–303.

40. Kraft, C. A., J. L. Garrido, …, G. Romero. 2009. Quantitative analysis of protein-lipid interactions using tryptophan fluorescence. *Sci. Signal.* 2:pl4.

41. Pande, A. H., S. Qin, and S. A. Tatulian. 2005. Membrane fluidity is a key modulator of membrane binding, insertion, and activity of 5-lipoxygenase. *Biophys. J.* 88:4084–4094.

42. Vanni, S., L. Vamparys, …, B. Antonny. 2013. Amphipathic lipid packing sensor motifs: probing bilayer defects with hydrophobic residues. *Biophys. J.* 104:575–584.

43. Krishnan, P., A. Singla, …, H. J. Wu. 2017. Hetero-multivalent binding of cholera toxin subunit B with glycolipid mixtures. *Colloids Surf. B Biointerfaces.* 160:281–288.

44. Wyman, J., and S. J. Gill. 1990. Chapter 3. The binding polynomial. Binding and Linkage: Functional Chemistry of Biological Macromolecules. University Science Books, p. xiii+330.

45. Atsumi, G., M. Murakami, …, I. Kudo. 1997. The perturbed membrane of cells undergoing apoptosis is susceptible to type II secretory phospholipase A2 to liberate arachidonic acid. *Biochim. Biophys. Acta.* 1349:43–54.

46. Murphy, E. J., L. Joseph, …, L. A. Horrocks. 1992. Phospholipid composition of cultured human endothelial cells. *Lipids.* 27:150–153.

47. Virtanen, J. A., K. H. Cheng, and P. Somerharju. 1998. Phospholipid composition of the mammalian red cell membrane can be rationalized by a superlattice model. *Proc. Natl. Acad. Sci. USA.* 95:4964–4969.

48. Zachowski, A. 1993. Phospholipids in animal eukaryotic membranes: transverse asymmetry and movement. *Biochem. J.* 294:1–14.

49. Lorent, J. H., K. R. Levental, …, I. Levental. 2020. Plasma membranes are asymmetric in lipid unsaturation, packing and protein shape. *Nat. Chem. Biol.* 16:644–652.

50. Jeppesen, B., C. Smith, …, J. F. Tait. 2008. Entropic and enthalpic contributions to annexin V-membrane binding: a comprehensive quantitative model. *J. Biol. Chem.* 283:6126–6135.

51. Gupta, A., T. Korte, …, T. Wohland. 2020. Plasma membrane asymmetry of lipid organization: fluorescence lifetime microscopy and correlation spectroscopy analysis. *J. Lipid Res.* 61:252–266.

52. Joo, F., F. Chevy, …, C. Wolf. 1993. The activation of rat platelets increases the exposure of polyunsaturated fatty acid enriched phospholipids on the external leaflet of the plasma membrane. *Biochim. Biophys. Acta.* 1149:231–240.

53. Gibbons, E., K. R. Pickett, …, J. D. Bell. 2013. Molecular details of membrane fluidity changes during apoptosis and relationship to phospholipase A(2) activity. *Biochim. Biophys. Acta.* 1828:887–895.

54. Van Blitterswijk, W. J., G. De Veer, …, P. Emmelot. 1982. Comparative lipid analysis of purified plasma membranes and shed extracellular membrane vesicles from normal murine thymocytes and leukemic GRSL cells. *Biochim. Biophys. Acta.* 688:495–504.

55. Ferber, E., G. G. De Pasquale, and K. Resch. 1975. Phospholipid metabolism of stimulated lymphocytes. Composition of phospholipid fatty acids. *Biochim. Biophys. Acta.* 398:364–376.

56. Goppelt-Strübe, M., and K. Resch. 1987. Polyunsaturated fatty acids are enriched in the plasma membranes of mitogen-stimulated T-lymphocytes. *Biochim. Biophys. Acta.* 904:22–28.

57. Anel, A., J. Naval, …, A. Piñeiro. 1990. Fatty acid metabolism in human lymphocytes. I. Time-course changes in fatty acid composition and membrane fluidity during blastic transformation of peripheral blood lymphocytes. *Biochim. Biophys. Acta.* 1044:323–331.

58. Leventis, P. A., and S. Grinstein. 2010. The distribution and function of phosphatidylserine in cellular membranes. *Annu. Rev. Biophys.* 39:407–427.

59. Lemmon, M. A. 2008. Membrane recognition by phospholipid-binding domains. *Nat. Rev. Mol. Cell Biol.* 9:99–111.

60. Lorizate, M., T. Sachsenheimer, …, B. Brügger. 2013. Comparative lipidomics analysis of HIV-1 particles and their producer cell membrane in different cell lines. *Cell Microbiol.* 15:292–304.

61. Kerr, D., G. T. Tietjen, …, K. Y. C. Lee. 2018. Sensitivity of peripheral membrane proteins to the membrane context: a case study of phosphatidylserine and the TIM proteins. *Biochim. Biophys. Acta Biomembr.* 1860:2126–2133.

62. Mosior, M., and S. McLaughlin. 1992. Electrostatics and reduction of dimensionality produce apparent cooperativity when basic peptides bind to acidic lipids in membranes. *Biochim. Biophys. Acta.* 1105:185–187.

63. Kwolek, U., W. Kulig, …, M. Kepczynski. 2015. Effect of phosphatidic acid on biomembrane: experimental and molecular dynamics simulations study. *J. Phys. Chem. B.* 119:10042–10051.

64. Dickey, A., and R. Faller. 2008. Examining the contributions of lipid shape and headgroup charge on bilayer behavior. *Biophys. J.* 95:2636–2646.

65. Kooijman, E. E., D. P. Tieleman, …, B. de Kruijff. 2007. An electrostatic/hydrogen bond switch as the basis for the specific interaction of phosphatidic acid with proteins. *J. Biol. Chem.* 282:11356–11364.

66. Shin, J. J. H., and C. J. R. Loewen. 2011. Putting the pH into phosphatidic acid signaling. *BMC Biol.* 9:85.

67. Loew, S., E. E. Kooijman, and S. May. 2013. Increased pH-sensitivity of protein binding to lipid membranes through the electrostatic-hydrogen bond switch. *Chem. Phys. Lipids.* 169:9–18.

68. Putta, P., J. Rankenberg, …, E. E. Kooijman. 2016. Phosphatidic acid binding proteins display differential binding as a function of membrane curvature stress and chemical properties. *Biochim. Biophys. Acta.* 1858:2709–2716.

69. Elmore, D. E. 2006. Molecular dynamics simulation of a phosphatidylglycerol membrane. *FEBS Lett.* 580:144–148.

70. Mukhopadhyay, P., L. Monticelli, and D. P. Tieleman. 2004. Molecular dynamics simulation of a palmitoyl-oleoyl phosphatidylserine bilayer with Na+ counterions and NaCl. *Biophys. J.* 86:1601–1609.

71. English, D. 1996. Phosphatidic acid: a lipid messenger involved in intracellular and extracellular signalling. *Cell. Signal.* 8:341–347.

72. Perry, D. K., V. L. Stevens, …, J. D. Lambeth. 1993. A novel ecto-phosphatidic acid phosphohydrolase activity mediates activation of neutrophil superoxide generation by exogenous phosphatidic acid. *J. Biol. Chem.* 268:25302–25310.

73. el Bawab, S., O. Macovschi, …, A. F. Prigent. 1995. Time-course changes in content and fatty acid composition of phosphatidic acid from rat thymocytes during concanavalin A stimulation. *Biochem. J.* 308:113–118.

74. Jenkins, G. M., and M. A. Frohman. 2005. Phospholipase D: a lipid centric review. *Cell. Mol. Life Sci.* 62:2305–2316.

75. Wang, X., S. P. Devaiah, …, R. Welti. 2006. Signaling functions of phosphatidic acid. *Prog. Lipid Res.* 45:250–278.

76. Bruntz, R. C., C. W. Lindsley, and H. A. Brown. 2014. Phospholipase D signaling pathways and phosphatidic acid as therapeutic targets in cancer. *Pharmacol. Rev.* 66:1033–1079.

77. Du, G., Y. M. Altshuller, …, M. A. Frohman. 2003. Regulation of phospholipase D1 subcellular cycling through coordination of multiple membrane association motifs. *J. Cell Biol.* 162:305–315.

78. Disse, J., N. Vitale, …, V. Gerke. 2009. Phospholipase D1 is specifically required for regulated secretion of von Willebrand factor from endothelial cells. *Blood.* 113:973–980.

79. Noh, J. Y., K. M. Lim, …, J. H. Chung. 2010. Procoagulant and prothrombotic activation of human erythrocytes by phosphatidic acid. *Am. J. Physiol. Heart Circ. Physiol.* 299:H347–H355.

80. Melendez, A. J., and J. M. Allen. 2002. Phospholipase D and immune receptor signalling. *Semin. Immunol.* 14:49–55.

81. Dahlgren, C., and A. Karlsson. 1999. Respiratory burst in human neutrophils. *J. Immunol. Methods.* 232:3–14.

82. Duffin, R., A. E. Leitch, …, A. G. Rossi. 2010. Targeting granulocyte apoptosis: mechanisms, models, and therapies. *Immunol. Rev.* 236:28–40.

83. Luo, H. R., and F. Loison. 2008. Constitutive neutrophil apoptosis: mechanisms and regulation. *Am. J. Hematol.* 83:288–295.

84. McPhail, L. C., K. A. Waite, …, S. Sergeant. 1999. A novel protein kinase target for the lipid second messenger phosphatidic acid. *Biochim. Biophys. Acta.* 1439:277–290.